A COST-EFFECTIVE METHOD FOR HIGH-QUALITY 60 GHZ OPTICAL MILLIMETER WAVE SIGNAL GENERATION BASED ON FREQUENCY QUADRUPLING

Nael A. Al-Shareefi[1, 4, *], Syed I. S. Hassan[2], Fareq Malek[2], Razali Ngah[3], Sura A. Abbas[4], and Syed A. Aljunid[1]

[1]School of Computer and Communication Engineering, Universiti Malaysia Perlis (UniMAP), Pauh Putra, Arau, Perlis 02600, Malaysia

[2]School of Electrical System Engineering, Universiti Malaysia Perlis (UniMAP), Pauh Putra, Arau, Perlis 02600, Malaysia

[3]Wireless Communication Centre, Faculty of Electrical Engineering, Universiti Teknologi Malaysia, Malaysia

[4]Ministry of Science and Technology, Directorate of Space Technology and Communications, Baghdad, Iraq

Abstract—In this paper, we present a cost effective method to generate a high-quality quadruple frequency optical millimeter-wave (MMW) signal using an integrated dual-parallel Mach-Zehnder modulator (IDP-MZM). Not only does the method minimize the complication of the central station (CS) and its frequency demand for the devices, but the generated optical MMW signal as well has good transmission performance. By properly adjusting the direct current (DC) bias, modulation index, and using two radio frequency (RF) driving signals with 135° phase delay, a high quality dual tone optical MMW at 60 GHz is generated from a 15 GHz RF local oscillator (LO) with optical sideband suppression ratio (OSSR) as high as 32 dB and radio frequency spurious suppression ratio (RFSSR) exceeding 33 dB without optical filter when an IDP-MZM with 30 dB extinction ratio is utilized. Furthermore, the influences of a number of non-ideal parameters, such as imperfect extinction ratio, non-ideal RF driven voltage, and phase difference of RF-driven signals applied to two sub-MZMs of the IDP-MZM, on OSSR are studied through simulation. Finally, we build a Radio over Fiber system through simulation, and the transmission performance of the generated optical MMW signal is

presented. The eye patterns still clear and keeps open even after 60 km transmission.

1. INTRODUCTION

Due to the rapid growth of broad-band internet services and business, MMW wireless access in the 60 GHz band becomes what the end-users need. However, Many difficulties in the 60 GHz wireless systems need to be solved, the most important is that the higher air-link loss. Another difficulty is that the 60 GHz band circuits are expensive and difficult to design and implement [1–6]. Radio over Fiber (RoF) technique, the integration of wireless and optical system, has long been proposed as an ideal technology for solving these difficulties since it can provide many advantages such as low propagation loss, low cost, large bandwidth and high transmission performance [7, 8]. In a RoF system, the cost-effective and high quality generation of high frequency MMW signals with simple implementation and low cost is a key technique that needs further development, especially for the frequency beyond 40 GHz [9–12]. The optical method is preferable over the conventional electrical method [13, 14]. Various techniques have been developed, such as the stimulated Brillouin scattering (SBS) in optical fiber [15], the use of four-wave mixing in a highly nonlinear fiber (HNLF) [16], and the optical frequency up-conversion using an external modulator, such as LiNbO$_3$ MZM [17–27]. Compared with these techniques, the optical frequency up-conversion technique could easily generate a stable MMW signal, because of good coherence of two or three generated optical sidebands.

Several different works have been recently reported to generate a pure optical MMW carrier by quadrupling the electrical RF LO carrier. Based on a 1×4 Multimode interference (MMI) coupler with four optical phase-modulator arms, Liu et al. demonstrated a novel technique to realize frequency quadrupling in the RoF system [28]. But the relative optical phase introduced by the MMI coupler needs an accurate tuning, which will require a complex control circuit to stabilize its operation. In [29], Zhao et al. used two cascaded MZMs to generate a quadruple frequency MMW signal. However, the undesired optical sidebands were not well eliminated. Thus, only a lower OSSR of 25 dB can be obtained, which degrades the RFSSR between the desired MMW signal and other undesired RF components. In [24], we proposed a new approach to generate quadrupling-frequency optical MMW signal with carrier suppression based on two parallel MZMs, where the OSSR value was about 40 dB.

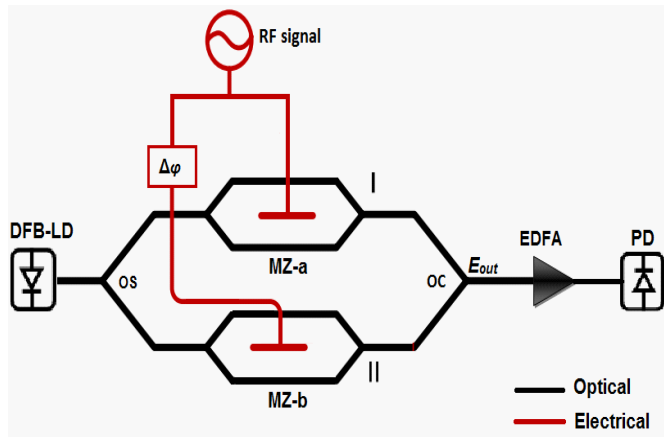In this paper, we propose a simple method to generate a

Figure 1. The principle of optical MMW generation using an IDP-MZM. (DFB-LD: distributed feedback laser diode; OS: optical splitter; OC: optical coupler; PD: photo diode; EDFA: erbium-doped fiber amplifier).

high quality quadruple frequency optical MMW using an IDP-MZM. Because the DP-MZM is a commercial off-the-shelf device fabricated on a single chip, our scheme enables the transmitter to have a compact structure, convenient alignment, and small insertion loss compared with other conventional transmitters. The modulation index will be adjusted and two RF driving signals with 135° phase delay will be applied to obtain an optical MMW signal with OSSR as high as 32 dB and RFSSR exceeding 33 dB when an IDP-MZM with extinction ratio (ER) of 30 dB is utilized. The influences of a number of non-ideal parameters on OSSR are studied through simulation. Finally, we build a RoF link through simulation to confirm the transmission performance of the generated optical MMW signal.

2. PRINCIPLE

The principle of optical MMW generation is shown in Figure 1. A continuous wave (CW) generated from a distributed feedback (DFB) laser diode is split into two branches, i.e., I and II by a 3-dB optical splitter. In each branch there is a single-electrode MZM, i.e., MZ-a in branch I and MZ-b in branch II. The two MZMs are integrated in the main MZM. The CW can be expressed as:

$$E_c(t) = E_c \exp(jw_c t) \tag{1}$$

where E_c is the amplitude of the optical field, and $w_c = 2\pi f_c$ is the angular frequency of the optical carrier. The RF-driven signal applied to MZ-a and MZ-b are:

$$V_a(t) = \frac{\sqrt{2}}{2} V_{\text{RF}} \sin(w_{\text{RF}} t) \quad V_b(t) = \frac{\sqrt{2}}{2} V_{\text{RF}} \sin(w_{\text{RF}} t + \Delta\phi) \quad (2)$$

where, V_{RF} and w_{RF} are, respectively, the amplitude and the angular frequency of the LO signal, and $\sqrt{2}$ is to regard the 3 dB electrical power splitter prior to the two MZMs. Another 3 dB electrical power splitter is also used prior to the two electrodes of every sub-MZM. Thus, the amplitude of RF-driven signal applied to the electrodes of MZM is $\frac{V_{\text{RF}}}{2}$. MZ-a and MZ-b are both biased at the maximum transmission point. An phase shift $\Delta\phi$ is introduced between the RF driving signals on MZ-a and MZ-b.

If the ER of the IDP-MZM is assumed to be infinite, i.e., ideal condition. The output optical signals from MZ-a can be mathematically expressed as:

$$E_{\text{MZ-}a}(t) = \frac{\alpha}{4} E_c e^{jw_c t} \left[e^{j \frac{\pi V_{\text{RF}}}{2V_\pi} \sin(w_{\text{RF}} t)} + e^{-j \frac{\pi V_{\text{RF}}}{2V_\pi} \sin(w_{\text{RF}} t)} e^{j \frac{\pi}{V_\pi} \cdot V_{dc}} \right]$$

$$= \frac{\alpha}{4} E_c e^{jw_c t} \left[e^{jm \sin(w_{\text{RF}} t)} + e^{-jm \sin(w_{\text{RF}} t)} \right] \quad (3)$$

By applying the Jaccobi-Anger expansion

$$e^{jm \sin(wt)} = \sum_{n=-\infty}^{\infty} J_n(m) e^{jnwt}, \quad e^{jm \cos(wt)} = \sum_{n=-\infty}^{\infty} j^n J_n(m) e^{jnwt} \quad (4)$$

on Equation (3), $E_{\text{MZ-}a}(t)$ becomes,

$$E_{\text{MZ-}a}(t) = \frac{\alpha}{4} E_c e^{jw_c t} \left[\sum_{n=-\infty}^{\infty} J_n(m) e^{j(nw_{\text{RF}} t)} + \sum_{n=-\infty}^{\infty} J_n(m) e^{j(nw_{\text{RF}} t + n\pi)} \right]$$

$$= \frac{\alpha}{4} E_c e^{jw_c t} \left[\sum_{n=-\infty}^{\infty} J_n(m) e^{j(nw_{\text{RF}} t + \frac{n\pi}{2} - \frac{n\pi}{2})} + \sum_{n=-\infty}^{\infty} J_n(m) e^{j(nw_{\text{RF}} t + \frac{n\pi}{2} + \frac{n\pi}{2})} \right]$$

$$= \frac{\alpha}{4} E_c e^{jw_c t} \left[\sum_{n=-\infty}^{\infty} J_n(m) e^{j(nw_{\text{RF}} t + \frac{n\pi}{2})} \left\{ e^{j(\frac{n\pi}{2})} + e^{-j(\frac{n\pi}{2})} \right\} \right]$$

$$= \frac{\alpha}{2} E_c \sum_{n=-\infty}^{\infty} J_n(m) \cos\left(\frac{n\pi}{2}\right) e^{j[(w_c + nw_{\text{RF}})t + \frac{n\pi}{2}]} \quad (5)$$

where α is the optical power loss within the IDP-MZM (Max. value is 5 dB), m the RF modulation index defined as $m = (\pi \cdot V_{\text{RF}}/2V_\pi)$, $J_n(\cdot)$ is the nth-order Bessel function of the first kind, and V_π the half-wave

voltage of the two sub-MZMs. In the same way, the output optical signals from MZ-b can be expressed as:

$$E_{\text{MZ-}b}(t) = \frac{\alpha}{2} E_c \sum_{n=-\infty}^{\infty} J_n(m) \cos\left(\frac{n\pi}{2}\right) e^{j[(w_c + nw_{\text{RF}})t + \frac{n\pi}{2} + n\Delta\phi]} \quad (6)$$

Thus, the optical field at the output of the optical coupler (OC) can be written as:

$$E_{out}(0, t) = E_{\text{MZ-}a}(t) + E_{\text{MZ-}b}(t)$$

$$E_{out}(0, t) = \frac{\alpha}{2} E_c \left[\sum_{n=-\infty}^{\infty} J_n(m) \cos\left(\frac{n\pi}{2}\right) e^{j\left[(w_c + nw_{\text{RF}})t + \frac{n\pi}{2}\right]} \right.$$

$$\left. + \sum_{n=-\infty}^{\infty} J_n(m) \cos\left(\frac{n\pi}{2}\right) e^{j\left[(w_c + nw_{\text{RF}})t + \frac{n\pi}{2} + n\Delta\phi\right]} \right]$$

$$= \frac{\alpha}{2} E_c \sum_{n=-\infty}^{\infty} [1 + e^{jn\Delta\phi}] J_n(m) \cos\left(\frac{n\pi}{2}\right) e^{j\left[(w_c + nw_{\text{RF}})t + \frac{n\pi}{2}\right]} \quad (7)$$

It is clear from Equation (7) that the odd-order sidebands are all suppressed because of $\cos(n\pi/2)$. So the $2k$th-order sidebands are generated at the output of the modulator, where k is an integer. To achieve quadruple frequency optical MMW with high OSSR, it is necessary that the second-order optical sidebands are maximized and the non-desired optical sidebands are suppressed. According to Equation (7), the zeroth-order and the fourth-order Bessel function becomes zero when the following conditions are met:

$$\begin{cases} J_0(m) = 0 & \text{when } m = 2.4048 \rightarrow V_{\text{RF}} = 1.5V_\pi \\ J_4(m) = 0 & \text{when } \Delta\phi = 45° \text{ or } 135° \end{cases} \quad (8)$$

Equation (8) is only valid for small-signal condition. It can be seen in Equation (8), that the optical carrier and fourth-order sidebands can be suppressed by adjusting the modulation index and introducing phase difference $\Delta\phi$ between the RF driven signal of MZ-a and MZ-b. Taking the characteristics of the Bessel function into consideration, the optical sidebands higher than the sixth-order can be neglected due to their extremely small power. Thus, Equation (7) can be approximately written as:

$$E_{out}(0, t) = \frac{\alpha}{2} E_c \left\{ J_2(2.4048) \left[e^{j[(w_c - 2w_{\text{RF}})t]} \left(1 + e^{-j2\Delta\phi}\right) \right. \right.$$

$$\left. + e^{j[(w_c + 2w_{\text{RF}})t]} \left(1 + e^{+j2\Delta\phi}\right) \right]$$

$$+ J_6(2.4048) \left[e^{j[(w_c - 6w_{\text{RF}})t]} \left(1 + e^{-j6\Delta\phi}\right) \right.$$

$$\left. \left. + e^{j[(w_c + 6w_{\text{RF}})t]} \left(1 + e^{+j6\Delta\phi}\right) \right] \right\} \quad (9)$$

here, $\Delta\phi$ equals 45° or 135°.

By utilizing Equation (9), the OSSR for IDP-MZM with infinite ER is given by:

$$\text{OSSR} = 10\log_{10}\left[\frac{J_2(2.4048)^2(1+\cos(2\Delta\phi))}{J_6(2.4048)^2(1+\cos(6\Delta\phi))}\right] = 42.07\,\text{dB} \qquad (10)$$

It is clear from Equation (10) that the OSSR is equal to 42.07 dB for both $\Delta\phi = 45°$ and $\Delta\phi = 135°$.

In a back-to-back (B-T-B) case, the quadrupling frequency optical MMW signal is detected by using a square-law PD, and its photocurrent can be expressed as:

$$I(0,t) = \mu\,|E_{out}(0,t)|^2 = \frac{\alpha^2}{4}\mu E_c^2\left[E_{out}(0,t)\times E_{out}(0,t)^*\right] \qquad (11)$$

where μ is the frequency response of the PD, and $E(0,t)^*$ represents the complex conjugate of $E(0,t)$. Equation (11) can be written, after manipulation, as: (see Appendix A)

$$I(0,t) = \frac{\alpha^2}{4}\mu E_c^2\left[\left\{2J_2^2(m)+4J_2(m)J_6(m)\right\}(1+\cos(2\Delta\phi))\cos(4w_{\text{RF}}t)\right.$$
$$+4J_2(m)J_6(m)(1+\cos(2\Delta\phi)+\cos(6\Delta\phi))\cos(8w_{\text{RF}}t)$$
$$\left.+2J_6^2(1+\cos(6\Delta\phi))\cos(12w_{\text{RF}}t)\right] \qquad (12)$$

It is clear from Equation (12) that the photocurrent contains the desired MMW signal at $4w_{\text{RF}}$, which we are interested in, and the harmonic distortion signals with frequency equal to $4nw_{\text{RF}}$, where $n < 2$. These MMW signal components are:

$$I_{4w_{\text{RF}}} = \frac{\alpha^2}{4}\mu E_c^2(1+\cos(2\Delta\phi))\cos(4w_{\text{RF}}t)\left\{2J_2^2(m)+4J_2(m)J_6(m)\right\}$$

$$I_{8w_{\text{RF}}} = \frac{\alpha^2}{4}\mu E_c^2(1+\cos(2\Delta\phi)+\cos(6\Delta\phi))\cos(8w_{\text{RF}}t)\{4J_2(m)J_6(m)\}$$

$$I_{12w_{\text{RF}}} = \frac{\alpha^2}{4}\mu E_c^2(1+\cos(6\Delta\phi))\cos(12w_{\text{RF}}t)\left\{2J_6^2\right\} \qquad (13)$$

By utilizing Equation (13), RFSSR can be written as:

$$\text{RFSSR} = 20\log_{10}\left[\frac{\left\{J_2^2(m)+2J_2(m)J_6(m)\right\}(1+\cos(2\Delta\phi))}{2J_2(m)J_6(m)(1+\cos(2\Delta\phi)+\cos(6\Delta\phi))}\right] = 34.3\,\text{dB}$$
$$(14)$$

It is clear from Equation (10) that the RFSSR is equal to 34.3 dB for both $\Delta\phi = 45°$ and $\Delta\phi = 135°$.

The generated optical MMW signals are transmitted over Z-length downlink fiber to the base station (BS), and the two second-order

sidebands will have different group velocities due to the fiber chromatic dispersion. The optical MMW signal becomes:

$$
\begin{aligned}
E(Z,t) = \frac{\alpha}{2} E_c e^{-\gamma Z} &\left\{ J_2(m) \left[e^{j[(w_c - 2w_{\mathrm{RF}})t - \beta(w_c - 2w_{\mathrm{RF}})Z]} \left(1 + e^{-j2\Delta\phi} \right) \right. \right. \\
&\left. + e^{j[(w_c + 2w_{\mathrm{RF}})t - \beta(w_c + 2w_{\mathrm{RF}})Z]} \left(1 + e^{+j2\Delta\phi} \right) \right] \\
&+ J_6(m) \left[e^{j[(w_c - 6w_{\mathrm{RF}})t - \beta(w_c - 6w_{\mathrm{RF}})Z]} \left(1 + e^{-j6\Delta\phi} \right) \right. \\
&\left.\left. + e^{j[(w_c + 6w_{\mathrm{RF}})t - \beta(w_0 + 6w_{\mathrm{RF}})Z]} \left(1 + e^{+j6\Delta\phi} \right) \right] \right\}
\end{aligned} \quad (15)
$$

where γ is the fiber loss, and $\beta(w)$ is the propagation constant of the fiber. By neglecting the sixth-order optical sidebands because of their extremely low power. The photocurrent can be express as follows:

$$
\begin{aligned}
I_{4w_{\mathrm{RF}}}(Z,t) = \mu \left| E(Z,t) \right|^2 = & \frac{\alpha^2}{2} \mu E_c^2 e^{-2\gamma Z} \\
& \left\{ J_2^2(m) + 2J_2(m)J_6(m) \right\} (1 + \cos(2\Delta\phi)) \\
& \cdot \left\{ \cos[4w_{\mathrm{RF}}t - \beta(w_c + 2w_{\mathrm{RF}})Z + \beta(w_c - 2w_{\mathrm{RF}})Z] \right\} (16)
\end{aligned}
$$

By considering the Taylor's expansion of the propagation constant $\beta(w_c \pm 2w_{RF})$

$$
\beta(w_c \pm 2w_{\mathrm{RF}}) = \beta(w_c) \pm 2w_{\mathrm{RF}}\beta'(w_c) + 2w_{\mathrm{RF}}^2 \beta''(w_c) \quad (17)
$$

where $\beta(w_c) = \frac{1}{v_g}$, $\beta''(w_c) = \frac{-D\lambda^2}{2\pi c}$, v_g denotes the group velocity, and D is the chromatic dispersion parameter. The photocurrent can be
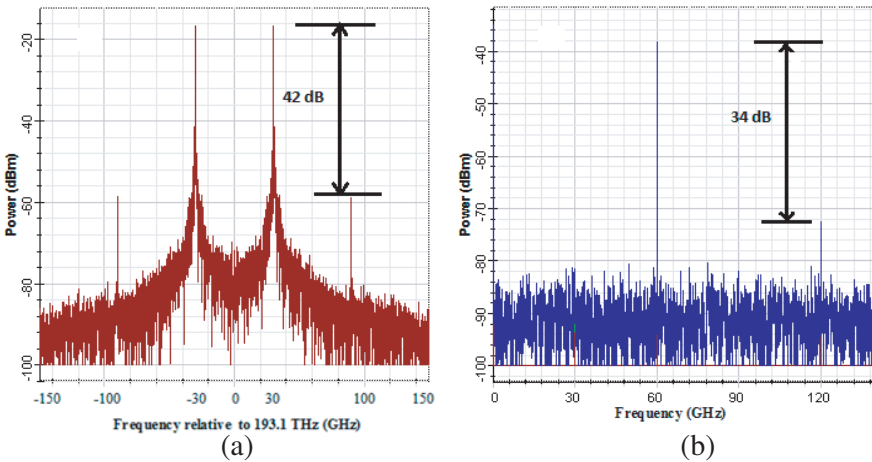

Figure 2. (a) Optical spectrum. (b) RF spectrum of the 60 GHz MMW signal at B-T-B case, when $\Delta\phi = 135°$ and the ER is infinite.

approximately express as:

$$I_{4w_{\mathrm{RF}}}(Z,t) = \frac{\alpha^2}{2}\mu E_c^2 e^{-2\gamma Z}\left\{J_2^2(m) + 2J_2(m)J_6(m)\right\}$$
$$(1 + \cos(2\Delta\phi)) \cdot \left\{\cos\left[4w_{\mathrm{RF}}(t - \beta^{'}(w_c)Z)\right]\right\} \quad (18)$$

Equation (18) clearly shows that the generated MMW at 60 GHz mainly consists of DC component and harmonic component at $4w_{\mathrm{RF}}$. Moreover, Equation (18) shows that the amplitude of the current for the desired MMW signal at $4w_{\mathrm{RF}}$ is independent of fiber dispersion. Therefore, the desired MMW signal is free from the drawback of the power fading induced by fiber dispersion. This condition applies if the desired MMW signal is generated by beating of the two second-order optical sidebands.

3. NUMERICAL SIMULATION RESULTS

3.1. Investigation the Quality of the Generated Optical MMW Signal Before Transmission over Fiber

In this section, the performance of the generated 60 GHz optical MMW signal is evaluated using "OptiSim Version 9.0" simulation software. The system is simulated as in Figure 1. A CW emitted from the DFB-LD with a linewidth of 10 MHz at a central wavelength of 1552.52 nm is sent to two sub-MZMs of the IDP-MZM. The two sub-MZMs are driven by the same RF LO of 15 GHz with a phase difference of 45° or 135° introduced by an electrical phase shifter between the RF-drive signal of MZ-a and MZ-b. The two sub-MZMs are identical with a switching voltage of $4v$ and insertion loss of 5 dB After the IDP-MZM, an EDFA with gain of 12 dB and noise figure of 5 dB is used for compensation for insertion loss of the optical modulator. For PD, $\Re = 0.7$ A/W, thermal noise is 1×10^{-11} A/HZ$^{0.5}$, and dark current is 2 nA.

Figure 2 shows the optical spectrum, and RF spectrum of the generated optical MMW, for $\Delta\phi = 135°$, when the ER of the IDP-MZM is 100 dB. It can be seen that the generated optical MMW mainly has two tones (positive and negative second-order sidebands) with a frequency spacing of 60 GHz, and the optical carrier and other undesired optical sidebands, except for the sixth-order sideband, are suppressed well. The power of the second-order sideband is -16 dBm and is noticeably higher than the power of the sixth-order sideband, and the OSSR is 42 dB, as shown in Figure 2(a). The RF spectrum mainly consists of the desired 60 GHz MMW signal and spurious 120 GHz MMW signal. However, the power of 60 GHz MMW signal

is higher than that of the 120 GHz MMW signal, and the RFSSR is 34 dB, as shown in Figure 2(b).

Figure 3 shows the optical spectrum, and RF spectrum of the generated optical MMW, for $\Delta\phi = 45°$, when the ER of the IDP-MZM is 100 dB. In this case, the OSSR and RFSSR are 42 dB and
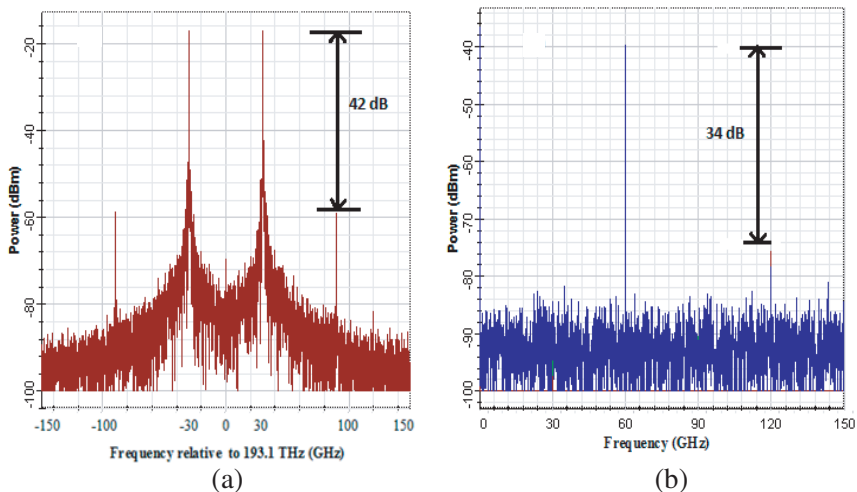

Figure 3. (a) Optical spectrum. (b) RF spectrum of the 60 GHz MMW signal at B-T-B case, when $\Delta\phi = 45°$ and the ER is infinite.
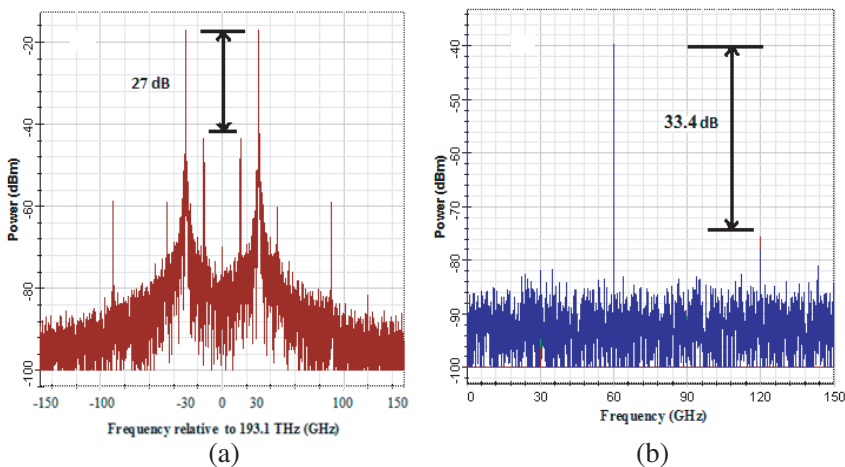

Figure 4. (a) Optical spectrum. (b) RF spectrum of the 60 GHz MMW signal at B-T-B case, when $\Delta\phi = 45°$ and the ER is 30 dB.
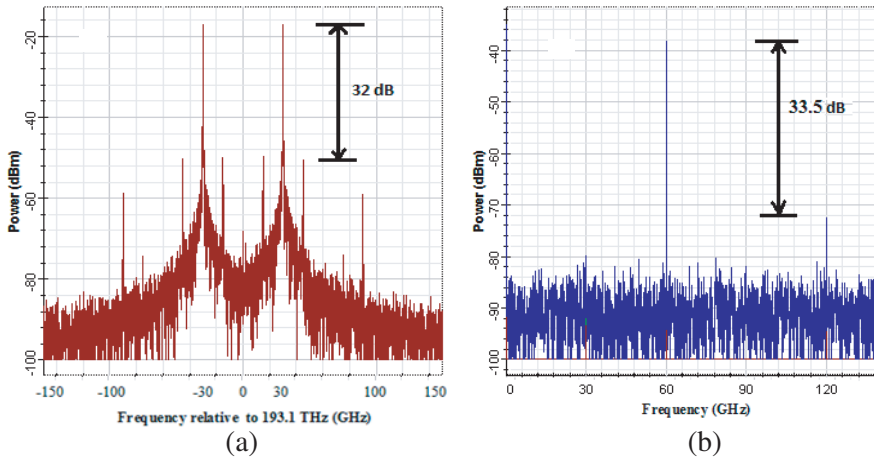
Figure 5. (a) Optical spectrum. (b) RF spectrum of the 60 GHz MMW signal at B-T-B case, when $\Delta\phi = 135°$ and the ER is 30 dB.

34 dB, respectively, and they are approximately identical to the values in Figure 2. Figure 2 and Figure 3 show that the simulation results are agree with the theoretical analysis in Section 2, Equations (10) and (14).

Figure 4 shows the optical spectrum, and RF spectrum of the generated optical MMW, for $\Delta\phi = 45°$, when the ER of the IDP-MZM is 30 dB. The power of the second-order sideband is maximum, and the OSSR exceeds 26 dB, as shown in Figure 4(a). The power of the 60 GHz MMW signal is clearly higher than the power of other spurious RF components, and RFSSR is as high as 33.4 dB, as shown in Figure 4(b).

The simulation results for $\Delta\phi = 135°$ and two sub-MZMs with ER of 30 dB are shown in Figure 5. Compared with the case of $\Delta\phi = 45°$, the undesired optical sidebands are further suppressed, the OSSR is as much as 32 dB and the RFSSR is 33.5 dB.

3.2. Investigation the Effect of Non-ideal Parameters on OSSR for B-T-B Case

The above theoretical derivation and simulation results are based on the assumption that system parameters such as RF driving voltage and phase difference are ideal. Initially, the OSSR can be unlimited, but in real systems, non-ideal factors contribute to a finite value. These conditions will result in the degradation of the generated optical MMW

signal. The quality of the MMW generation may be also affected. Therefore, investigating the influence of these non-ideal parameters is important. Except for the ER of the IDP-MZM, RF-driven voltage, and the phase difference between RF-driven signals applied to MZ-a and MZ-b, other parameters are identical to those given in Section 3.1.

Figure 6 shows the effect of phase shift deviation on OSSR. The highest OSSR can be obtained for a phase difference near the ideal value. The value then slightly degrades with the increment of deviation value for two cases, i.e., $\Delta\phi = 45°$ or $\Delta\phi = 135°$. An OSSR greater than 21 dB can be obtained for $\Delta\phi = 135°$ if the deviation is within $10°$, which is a desirable result.

The impact of non-ideal drive voltage of RF-driven signal on OSSR is shown in Figure 7. The variation of the OSSR versus the deviation of the driven voltage is identical. The OSSR greater than 19 dB can be obtained for $\Delta\phi = 135°$ if the deviation is less than 8%.

Figure 8 shows the variation of OSSR versus the imperfect ER of the IDP-MZM for $\Delta\phi = 45°$ and $\Delta\phi = 135°$. It can be seen that OSSR is better in the case when $\Delta\phi = 135°$. The OSSR reaches its maximum value when the ER is 40 dB, while when $\Delta\phi = 45°$ the OSSR reaches its maximum value when the ER is 50 dB and then retains unchangeable.

3.3. Investigation the Quality of the Generated Optical MMW Signal Over Fiber

In this section, we build a RoF system through simulation to confirm the transmission performance of the generated optical MMW signal, as shown in Figure 9. The identical parameters is used for the
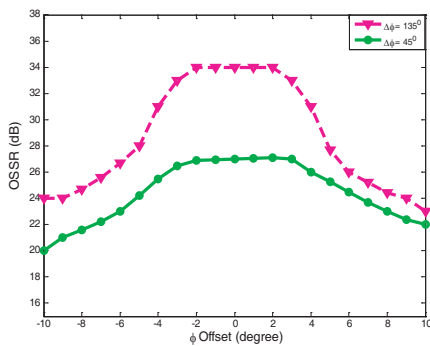

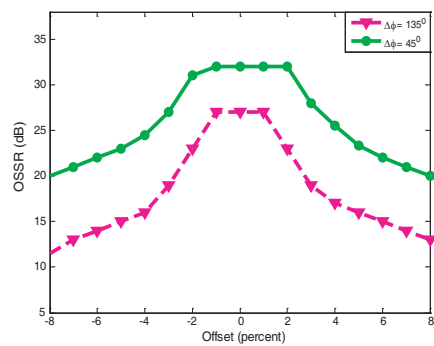**Figure 6.** OSSR against phase shift deviation at an ER of 30 dB.

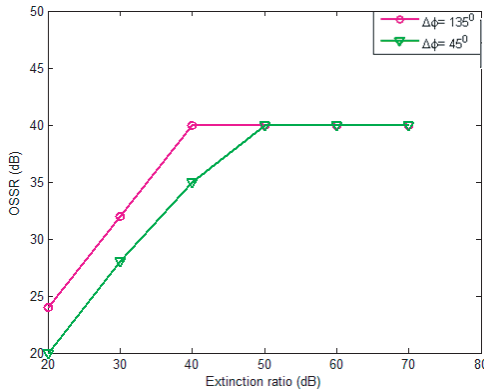**Figure 7.** OSSR against RF driving voltage deviation at an ER of 30 dB.

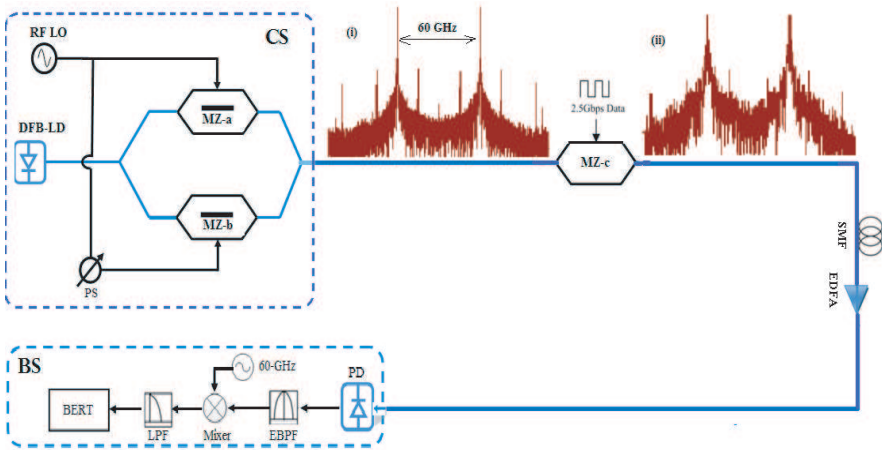**Figure 8.** The impact of imperfect ER on OSSR.

Figure 9. Simulation setup for the RoF system. (SMF: single-mode fiber; EBPF: electrical bandpass filter; LPF: lowpass filter; BERT: bit error rate tester).

identical components in Figure 1. The simulation was carried out at a rate of 2.5 Gbit/s over different distance with the ITU-T G.652 standard single-mode optical fiber (SSMF). All the attenuation (i.e., $\alpha = 0.23$ dB/km), dispersion (i.e., $D = 16.7$ ps/nm km), and non linear effect such as self phase modulation was activated and specified in accordance with the typical industry standards to simulate the real environment as close as possible.

After the proposed quadruple frequency MMW generation scheme,

two second-order sidebands are generated and maximised, and the frequency spacing between them is 60 GHz, as shown in Figure 9(i). The two second-order sidebands are then intensity modulated with a 2.5 Gbit/s baseband signal by another MZM (MZ-c) with an ER of 30 dB, as shown in Figure 9(ii). Figure 9(ii) shows that the second-order optical sidebands are broadened by signal modulation and attenuated by the modulator insertion loss. At the base station, a PD detects the quadruple frequency optical MMW, and an electrical 1st-order Gaussian bandpass filter centered at 60 GHz filters out the RF harmonics. To demodulate the 2.5 Gbit/s signal from the
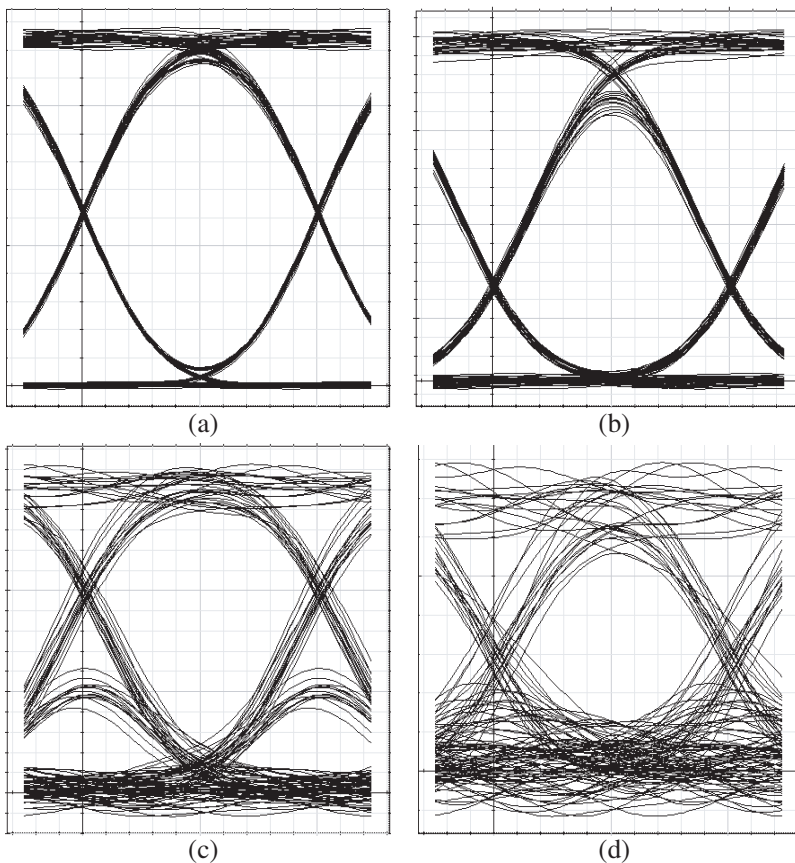

(a)

(b)

(c)

(d)

Figure 10. The eye patterns of 2.5 Gbit/s binary baseband signal of the optical MMW by simulation at (a) B-T-B, (b) 20 km, (c) 40 km, and (d) 60 km.
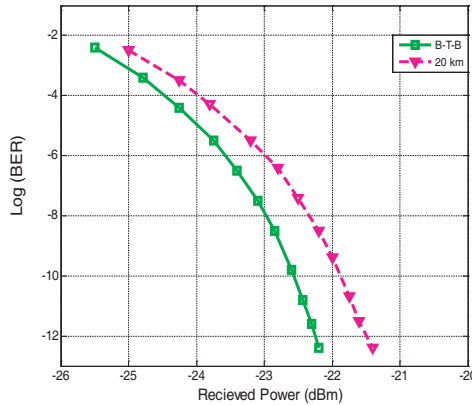
Figure 11. BER versus received optical power for the generation of optical MMW signals at 60 GHz at the transmission distance of 0 km and 20 km.

generated 60 GHz MMW signal, a 60 GHz RF LO, a mixer, and an electrical lowpass filter with a bandwidth of 2.8 GHz are utilised. The performance of the system was characterized by referring to the bit error rate (BER) and eye pattern.

Figure 10 shows the down-converted 2.5 Gbit/s electrical eye patterns of the 60 GHz MMW, for $\Delta\phi = 135°$, after transmission over different distance. It can be seen that the outline of the eye patterns changes slightly and the eye patterns still clear and keeps open even when the optical MMW signals are transmitted over 60 km transmission. The simulated BER performance of the RoF system is presented in Figure 11. It is indicated from Figure 11 that after 20 km transmission, the power penalty is about 0.75 dB at the BER of 10^{-9}. The power penalty is resulting essentially from the walk-off time, due to fiber chromatic dispersion, between the two optical harmonics [30]. and thus, the performance of the generated MMW signal is acceptable.

4. CONCLUSION AND FUTURE WORK

In this paper, we have presented a cost-effective method to generate a high-quality quadruple frequency optical MMW signal using only one IDP-MZM, and have investigated its transmission performance along a Standard Single-Mode Fiber.

The conclusions can be summarized as follows:

- This method can: (1) reduce the complexity of the central station and its frequency requirement for the devices; (2) generate

optical MMW signal that has good transmission performance and does not suffer from power fading induced by fiber dispersion, but cannot mitigate the walk-off effect, due to fiber chromatic dispersion, after 60 km transmission distance.

- The frequency quadrupling is achieved by adjusting the modulation index, and using two values for the phase difference (i.e., $\Delta\phi = 45°$ and $135°$) between the RF driven signal of MZ-a and MZ-b, but best performance is demonstrated when $\Delta\phi$ is equals $135°$.
- The influence of non-ideal parameters on OSSR is investigated by simulation. Results indicate that the slightly deviation of the ideal values would not cause large degradation of the generated optical MMW signal.
- Future works should focus on decreasing the walk-off effect by using a new methods based on modulating the based band signal on one tone of the optical MMW signal.

APPENDIX A.

Derivation of Eq. (12).

In B-T-B case, the quadruple frequency optical MMW signal is detected by a square-law photodiode (PD), and its photocurrent can be written as:

$$I(0,t) = \mu \left|E(0,t)\right|^2 = \mu \frac{\alpha^2}{4} E_c^2 \left[E(0,t) \times E(0,t)^*\right]$$

$$= \mu \frac{\alpha^2}{4} E_c^2 \left[J_2(m)e^{j[(w_c - 2w_{\mathrm{RF}})t]} \left(1 + e^{-j2 \cdot \Delta\phi}\right) \right.$$

$$+ J_2(m)e^{j[(w_c + 2w_{\mathrm{RF}})t]} \left(1 + e^{+j2 \cdot \Delta\phi}\right)$$

$$+ J_6(m)e^{j[(w_c - 6w_{\mathrm{RF}})t]} \left(1 + e^{-j6 \cdot \Delta\phi}\right)$$

$$\left. + J_6(m)e^{j[(w_c + 6w_{\mathrm{RF}})t]} \left(1 + e^{+j6 \cdot \Delta\phi}\right)\right]$$

$$\cdot \left[J_2(m)e^{-j[(w_c - 2w_{\mathrm{RF}})t]} \left(1 + e^{+j2 \cdot \Delta\phi}\right)\right.$$

$$+ J_2(m)e^{-j[(w_c + 2w_{\mathrm{RF}})t]} \left(1 + e^{-j2 \cdot \Delta\phi}\right)$$

$$+ J_6(m)e^{-j[(w_c - 6w_{\mathrm{RF}})t]} \left(1 + e^{+j6 \cdot \Delta\phi}\right)$$

$$\left. + J_6(m)e^{-j[(w_c + 6w_{\mathrm{RF}})t]} \left(1 + e^{-j6 \cdot \Delta\phi}\right)\right] \tag{A1}$$

where μ is the frequency response of the PD, $J_n(m)$ is the n-th order Bessel function of the first kind and $E(0,t)^*$ stands for complex

conjugate of $E(0,t)$. Eq. (A1) can be further simplified to:

$$
\begin{aligned}
I(0,t) = \mu \frac{\alpha^2}{4} E_c^2 \Big[&J_2^2(2 + 2\cos(2\Delta\phi)) \\
&+ J_2^2 e^{j[(w_c - 2w_{\mathrm{RF}} - w_c - 2w_{\mathrm{RF}})t]} \left(1 + 2e^{-j2\cdot\Delta\phi} + e^{-j4\cdot\Delta\phi} \right) \\
&+ J_2 J_6 e^{j[(w_c - 2w_{\mathrm{RF}} - w_c + 6w_{\mathrm{RF}})t]} \left(1 + e^{j6\Delta\phi} + e^{-j2\Delta\phi} + e^{j4\Delta\phi} \right) \\
&+ J_2 J_6 e^{j[(w_c - 2w_{\mathrm{RF}} - w_c - 6w_{\mathrm{RF}})t]} \left(1 + e^{-j6\Delta\phi} + e^{-j2\Delta\phi} + e^{-j8\Delta\phi} \right) \\
&J_2^2(2 + 2\cos(2\Delta\phi)) + J_2^2 e^{j[(w_c + 2w_{\mathrm{RF}} - w_c + 2w_{\mathrm{RF}})t]} \left(1 + 2e^{j2\cdot\Delta\phi} + e^{j4\cdot\Delta\phi} \right) \\
&+ J_2 J_6 e^{j[(w_c + 2w_{\mathrm{RF}} - w_c + 6w_{\mathrm{RF}})t]} \left(1 + e^{j6\Delta\phi} + e^{j2\Delta\phi} + e^{j8\Delta\phi} \right) \\
&+ J_2 J_6 e^{j[(w_c + 2w_{\mathrm{RF}} - w_c - 6w_{\mathrm{RF}})t]} \left(1 + e^{-j6\Delta\phi} + e^{j2\Delta\phi} + e^{-j4\Delta\phi} \right) \\
&+ J_6^2(2 + 2\cos(6\Delta\phi)) + J_6^2 e^{j[(w_c - 6w_{\mathrm{RF}} - w_c - 6w_{\mathrm{RF}})t]} \\
&\left(1 + 2e^{-j6\cdot\Delta\phi} + e^{-j12\cdot\Delta\phi} \right) \\
&+ J_2 J_6 e^{j[(w_c - 6w_{\mathrm{RF}} - w_c + 2w_{\mathrm{RF}})t]} \left(1 + e^{j2\Delta\phi} + e^{-j6\Delta\phi} + e^{-j4\Delta\phi} \right) \\
&+ J_2 J_6 e^{j[(w_c - 6w_{\mathrm{RF}} - w_c - 2w_{\mathrm{RF}})t]} \left(1 + e^{-j2\Delta\phi} + e^{-j6\Delta\phi} + e^{-j8\Delta\phi} \right) \\
&+ J_6^2(2 + 2\cos(6\Delta\phi)) + J_6^2 e^{j[(w_c + 6w_{\mathrm{RF}} - w_c + 6w_{\mathrm{RF}})t]} \\
&\left(1 + 2e^{j6\cdot\Delta\phi} + e^{j12\cdot\Delta\phi} \right) \\
&+ J_2 J_6 e^{j[(w_c + 6w_{\mathrm{RF}} - w_c + 2w_{\mathrm{RF}})t]} \left(1 + e^{j2\Delta\phi} + e^{j6\Delta\phi} + e^{j8\Delta\phi} \right) \\
&+ J_2 J_6 e^{j[(w_c + 6w_{\mathrm{RF}} - w_c - 2w_{\mathrm{RF}})t]} \left(1 + e^{-j2\Delta\phi} + e^{j6\Delta\phi} + e^{j4\Delta\phi} \right) \quad \text{(A2)}
\end{aligned}
$$

$$
\begin{aligned}
= \mu \frac{\alpha^2}{4} E_c^2 \Big[&J_2^2(2 + 2\cos(2\Delta\phi)) + J_2^2 e^{-j4w_{\mathrm{RF}}t} \left(1 + 2e^{-j2\cdot\Delta\phi} + e^{-j4\cdot\Delta\phi} \right) \\
&+ J_2 J_6 e^{j4w_{\mathrm{RF}}t} \left(1 + e^{j6\Delta\phi} + e^{-j2\Delta\phi} + e^{j4\Delta\phi} \right) \\
&+ J_2 J_6 e^{-j8w_{\mathrm{RF}}t} \left(1 + e^{-j6\Delta\phi} + e^{-j2\Delta\phi} + e^{-j8\Delta\phi} \right) \\
&J_2^2(2 + 2\cos(2\Delta\phi)) + J_2^2 e^{j4w_{\mathrm{RF}}t} \left(1 + 2e^{j2\cdot\Delta\phi} + e^{j4\cdot\Delta\phi} \right) \\
&+ J_2 J_6 e^{j8w_{\mathrm{RF}}t} \left(1 + e^{j6\Delta\phi} + e^{j2\Delta\phi} + e^{j8\Delta\phi} \right) \\
&+ J_2 J_6 e^{-j4w_{\mathrm{RF}}t} \left(1 + e^{-j6\Delta\phi} + e^{j2\Delta\phi} + e^{-j4\Delta\phi} \right)
\end{aligned}
$$

$$+J_6^2(2+2\cos(6\Delta\phi)) + J_6^2 e^{j-12w_{\mathrm{RF}}t}\left(1+2e^{-j6\cdot\Delta\phi} + e^{-j12\cdot\Delta\phi}\right)$$

$$+J_2 J_6 e^{-j4w_{\mathrm{RF}}t}\left(1 + e^{j2\Delta\phi} + e^{-j6\Delta\phi} + e^{-j4\Delta\phi}\right)$$

$$+J_2 J_6 e^{-j8w_{\mathrm{RF}}t]}\left(1 + e^{-j2\Delta\phi} + e^{-j6\Delta\phi} + e^{-j8\Delta\phi}\right)$$

$$+J_6^2(2 + 2\cos(6\Delta\phi)) + J_6^2 e^{j12w_{\mathrm{RF}}t}\left(1 + 2e^{j6\cdot\Delta\phi} + e^{j12\cdot\Delta\phi}\right)$$

$$+J_2 J_6 e^{j8w_{\mathrm{RF}}t}\left(1 + e^{j2\Delta\phi} + e^{j6\Delta\phi} + e^{j8\Delta\phi}\right)$$

$$+J_2 J_6 e^{j4w_{\mathrm{RF}}t}\left(1 + e^{-j2\Delta\phi} + e^{j6\Delta\phi} + e^{j4\Delta\phi}\right) \tag{A3}$$

$$I(0,t) = \mu\frac{E_0^2}{4}\Big[2J_2^2(1 + \cos(2\Delta\phi)) + 2J_6^2(1 + \cos(6\Delta\phi))$$

$$+2J_2^2(1+\cos(2\Delta\phi))\cos(4w_{\mathrm{RF}}t)+4J_2 J_6(1+\cos(2\Delta\phi))\cos(4w_{\mathrm{RF}}t)$$

$$+4J_2 J_6(1 + \cos(2\Delta\phi) + \cos(6\Delta\phi))\cos(8w_{\mathrm{RF}}t)$$

$$+2J_6^2(1 + \cos(6\Delta\phi))\cos(12w_{\mathrm{RF}}t) \tag{A4}$$

$$= \mu\frac{E_0^2}{4}\Big[\left\{2J_2^2(m) + 4J_2(m)J_6(m)\right\}(1 + \cos(2\Delta\phi))\cos(4w_{\mathrm{RF}}t)$$

$$+4J_2(m)J_6(m)(1 + \cos(2\Delta\phi) + \cos(6\Delta\phi))\cos(8w_{\mathrm{RF}}t)$$

$$+2J_6^2(1 + \cos(6\Delta\phi))\cos(12w_{\mathrm{RF}}t)\Big] \tag{A5}$$

This is Eq. (12).

REFERENCES

1. Anang, K. A., P. B. Rapajic, L. Bello, and R. Wu, "Sensitivity of cellular wireless network performance to system & propagation parameters at carrier frequencies greater than 2 GHz," *Progress In Electromagnetics Research B*, Vol. 40, 31–54, 2012.

2. Huang, T.-Y. and T.-J. Yen, "A high-ratio bandwidth square-wave-like bandpass filter by two-handed metamaterials and its application in 60 GHZ wireless communication," *Progress In Electromagnetics Research Letters*, Vol. 21, 19–29, 2011.

3. Sarrazin, T., H. Vettikalladi, O. Lafond, M. Himdi, and N. Rolland, "Low cost 60 GHz new thin Pyralux membrane antennas fed by substrate integrated waveguide," *Progress In Electromagnetics Research B*, Vol. 42, 207–224, 2012.

4. Navarro-Cía, M., V. Torres Landivar, M. Beruete, and M. Sorolla Ayza, "A slow light fishnet-like absorber in the millimeter-wave range," *Progress In Electromagnetic Research*, Vol. 118, 287–301, 2011.

5. Kapilevich, B. and B. Litvak, "Noise versus coherency in MM-wave and microwave scattering from nonhomogeneous materials," *Progress In Electromagnetics Research B*, Vol. 28, 35–54, 2011.

6. Deruyck, M., W. Vereecken, W. Joseph, B. Lannoo, M. Pickavet, and L. Martens, "Reducing the power consumption in wireless access networks: Overview and recommendations," *Progress In Electromagnetics Research*, Vol. 132, 255–274, 2012.

7. Ogawa, H. and D. Polifko, "Fiber optic millimeter-wave subcarrier transmission links for personal radio communication systems," *IEEE MTT-S International Microwave Symposium Digest*, 555–558, 1992.

8. Lu, H.-H., C.-Y. Li, C.-H. Lee, Y.-C. Hsiao, and H.-W. Chen, "Radio-over-fiber transport systems based on DFB LD with main and −1 side modes injection-locked technique," *Progress In Electromagnetics Research Letters*, Vol. 7, 25–33, 2009.

9. Chun, T., Lin, J. Chen, W. Q. Xue, P. C. Peng, and S. Chi, "Optical millimeter-wave signal generation using frequency quadrupling technique and no optical filtering, *IEEE Photonics Technology Letters*, Vol. 20, No. 12, 1027–1029, 2008.

10. Kotb, H. E., M. Y. Shalaby, and M. H. Ahmed, "Generation of nanosecond optical pulses with controlled repetition rate using in-cavity intensity modulated brillouin erbium fiber laser," *Progress In Electromagnetics Research*, Vol. 113, 313–331, 2011.

11. Calo, G., D. Alexandropoulos, and V. Petruzzelli, "Active WDM filter on dilute nitride quantum well photonic band gap waveguide," *Progress In Electromagnetics Research Letters*, Vol. 35, 37–49, 2012.

12. Jia, Z., et al., "Key enabling technologies for optical wireless networks: Optical millimeter-wave generation, wavelength reuse, and architecture," *Journal of Lightwave Technology*, Vol. 25, 3452–3471, 2007.

13. Kumar, A., B. Suthar, V. Kumar, K. S. Singh, and A. Bhargava, "Tunable wavelength demultiplexer for DWDM application using 1-D photonic crystal," *Progress In Electromagnetics Research Letters*, Vol. 33, 27–35, 2012.

14. Kapilevich, B. and B. Litvak, "Noise versus coherency in MM-wave and microwave scattering from nonhomogeneous materials," *Progress In Electromagnetics Research B*, Vol. 28, 35–54, 2011.

15. Park, C., C. G. Lee, C. S. Park, "Photonic frequency Up conversion by SBS-based frequency tripling," *Journal of Lightwave Technology*, Vol. 25, No. 7, 1711–1718, 2007.

16. Wang, Q., H. Rideout, F. Zeng, and J. Yao, "Millimeter-wave frequency tripling based on four-wave mixing in a semiconductor optical amplifier," *IEEE Photonics Technology Letters*, Vol. 18, No. 23, 2460–2462, 2006.

17. Yu, J., Z. Jia, L. Yi, Y. Su, G. K. Chang, T. and Wang, "Optical millimeter-wave generation or up-conversion using external modulators," *IEEE Photonics Technology Letters*, Vol. 18, No. 1, 265–267, 2006.

18. Liu, J., L. Zhang, S.-H. Fan, C. Guo, S. He, and G.-K. Chang, "A novel architecture for peer-to-peer interconnect in millimeter-wave radio-over-fiber access networks," *Progress In Electromagnetics Research*, Vol. 126, 139–148, 2012.

19. Shi, P., et al., "A frequency sextupling scheme for high-quality optical millimeter-wave signal generation without optical filter," *Optical Fiber Technology*, Vol. 17, 236–241, 2011.

20. Zhang, J., H. Chen, M. Chen, T. Wang, and S. Xie, "A photonic microwave frequency quadrupler using two cascaded intensity modulators with repetitious optical carrier suppression," *IEEE Photonics Technology Letters*, Vol. 19, No. 14, 1057–1059, 2007.

21. Deng, L., D. Liu, X. Pang, X. Zhang, V. Arlunno, Y. Zhao, A. Caballero, A. K. Dogadaev, X. Yu, I. T. Monroy, M. Beltran, and R. Llorente, "42.13 Gbit/S 16QAM-OFDM photonics-wireless transmission in 75–110 GHz band," *Progress In Electromagnetics Research*, Vol. 126, 449–461, 2012.

22. Qi, G., J. Yao, J. Seregelyi, S. Paquet, and C. Bélisle, "Optical generation and distribution of continuously tunable millimeter-wave signals using an optical phase modulator," *Journal of Lightwave Technology*, Vol. 23, No. 9, 2687–2695, 2005.

23. Shi, P., S. Yu, et al., "A novel frequency sextupling scheme for optical mm-wave generation utilizing an integrated dual-parallel Mach-Zehnder modulator," *Optics Communications*, Vol. 283, No. 19, 3667–3672, 2010.

24. Al-Shareefi, N. A., S. H. Idris, M. F. B. A. Malek, R. Ngah, S. A. Aljunid, R. A. Fayadh, J. Adhab, and H. A. Rahim, "Development of a new approach for high-quality quadrupling frequency optical millimeter-wave signal generation without optical filter," *Progress In Electromagnetics Research*, Vol. 134, 189–208, 2012.

25. Chen, L., H. Wen, and S. Wen, "A radio-over-fiber system with a novel scheme for millimeter-wave generation and wavelength reuse for up-link connection," *IEEE Photonics Technology Letters*, Vol. 18, No. 19, 2056–2058, 2006.

26. Zavargo-Peche, L., A. Ortega-Monux, J. G. Wanguemert-Perez,

and I. Molina-Fernandez, "Fourier based combined techniques to design novel sub-wavelength optical integrated devices," *Progress In Electromagnetics Research*, Vol. 123, 447–465, 2012.

27. He, J., L. Chen, Z. Dong, S. Wen, and J. Yu, "Full-duplex radio-over-fiber system with photonics frequency quadruples for optical millimeter-wave generation," *Optical Fiber Technology*, Vol. 15, No. 3, 290–295, 2009.

28. Liu, X., et al., "Frequency quadrupling using an integrated Mach-Zehnder modulator with four arms," *Optics Communications*, Vol. 284, 4052–4058, 2011.

29. Zhao, Y., et al., "Simplified optical millimeter-wave generation configuration by frequency quadrupling using two cascaded Mach-Zehnder modulators," *Optics Letters*, Vol. 34, 3250–3252, 2009.

30. Ma, J., et al., "Fiber dispersion influence on transmission of the optical millimeter-waves generated using LN-MZM intensity modulation," *Journal of Lightwave Technology*, Vol. 25, 3244–3256, 2007.